Magnetic Phase Transition of Ultrathin Fe Films on Ag(111)

Z. Q. Qiu, J. Pearson, and S. D. Bader
Materials Science Division, Argonne National Laboratory, Argonne, Illinois 60439
(Received 2 July 1991)

High-quality, single-crystalline films of Fe(110)/Ag(111) were grown by molecular-beam epitaxy in the range of ~1–3 monolayers of Fe, and investigated *in situ* by means of the surface magneto-optic Kerr effect. The magnetization exhibits a second-order phase transition at a thickness-dependent Curie temperature. The value of the critical exponent β of 0.137 ± 0.008 is in good agreement with that of the two-dimensional Ising model.

PACS numbers: 75.40.Cx, 05.70.Jk, 75.70.Ak

The investigation of two-dimensional (2D) magnetic systems has attracted great attention in recent years [1]. One of the most important topics concerns the critical behavior at the phase transition. While it is well known that for an isotropic 2D Heisenberg model [2] ordering occurs at 0 K, the introduction of anisotropy into the problem permits finite-temperature ordering to occur [3]. As the thickness of a ferromagnetic film is reduced, a decrease in the Curie temperature T_C is expected. It is generally accepted that the system undergoes a second-order transition at T_C and that the magnetization M follows a universal power law: $M = M_0(1 - T/T_C)^{\beta_c}$, where β_c is the critical exponent. Theory predicts that the critical exponent β_c will take on a value that depends on the universality class, and that in 2D β_c is $\frac{1}{8}$, $\frac{1}{9}$, and $\frac{1}{12}$ for two-, three-, and four-state Potts models, respectively [4]. The two-state Potts model is better known as the famous Ising model [5]. It also is known that four-, five-, and six-state clock models exhibit Ising transitions [6]. Other 2D possibilities that have been explored include the isotropic XY model, which has a Kosterlitz-Thouless transition [7], and the XY model with cubic anisotropy [8], which has a nonuniversal exponent that depends on the strength of the anisotropy.

Experimental investigations of 2D magnetic overlayers have benefited from the development of molecular-beam epitaxy (MBE), which permits atomic-scale control of the growth of high-quality, single crystals. Various measurement techniques [9] have been applied to study 2D phase transitions, and, as anticipated, reduced T_C values compared with the corresponding bulk value have been reported [10–12]. However, experimental determinations of the effective critical exponent β have produced controversial results. For example, the Fe(100)/Pd(100) [12] and V(100)/Ag(100) [13] systems yield β values of $\frac{1}{8}$, while Fe(100)/Au(100) [11], Tb(0001)/W(110) [13], and Ni(111)/Cu(111) [14] yield values of 0.22, 0.35, and 0.24, respectively. The latter values are significantly outside the range of expectation, unless they are nonuniversal and/or not characteristic of the 2D critical region. Further controversy stems from conflicting reports that V/Ag(100) is not magnetic [15], and that Fe/Au(100) has interdiffusional problems [16] that alter the magnitude and direction of the surface magnetic anisotropy. Also, transition-metal substrates offer the additional complexity of strong d-band hybridization across the interface. For Fe/Pd(100) this leads to significant induced moments on the interfacial Pd [17]. While the transition for Fe/Pd(100) remains Ising class [12], the role of the magnetic Pd layer in the phase transition is a relatively unexplored problem in statistical mechanics. Clearly, the experimental situation requires further study with a proper choice of system. We use the Fe(110)/Ag(111) system because it has the following advantages: (i) Fe and Ag are immiscible, which inhibits alloying and interdiffusion at the interface, and yields a thermally reversible magnetization; (ii) the d electrons of Fe hybridize weakly with the sp valence electrons of Ag [18], so that ultrathin films of Fe on Ag form an almost ideal 2D ferromagnetic system; and (iii) the system is relatively well studied in the literature [19,20].

First we present the results of the growth and characterization of Fe(110) on Ag(111). We then report on the temperature dependence of the magnetization and the thickness dependence of T_C in the range of 1–3 monolayers (ML) Fe, based on surface magneto-optic Kerr-effect (SMOKE) measurements. We find that (i) Fe(110) grows epitaxially on Ag(111) in a layer-by-layer fashion; (ii) in the monolayer range, the T_C value of Fe(110) on Ag(111) is significantly reduced compared to the bulk value; (iii) the magnetization shows a second-order phase transition at T_C and obeys the expected power law with an effective β value of 0.137 ± 0.008, which is close to the value of $\frac{1}{8}$ for the 2D Ising model.

The Fe(110)/Ag(111) films were prepared by MBE in a new ultrahigh vacuum (UHV) chamber of base pressure 1×10^{-10} Torr. The system is equipped with reflection high-energy electron diffraction (RHEED), low-energy electron diffraction (LEED), Auger spectroscopy using a hemispherical analyzer with a mean radius of 140 mm, Ar-ion sputtering, and a split-coil, UHV-compatible superconducting magnet. Cleaved mica serves as the starting substrate for film growth. The mica was ultrasonically cleaned in methanol, introduced into UHV, and annealed at 700 K for 12 h. A Ag(111) base layer was then deposited onto the mica from a Ag foil in an alumina crucible. The mica was held at 450 K during deposition and the deposition rate was ~0.5 Å/min.

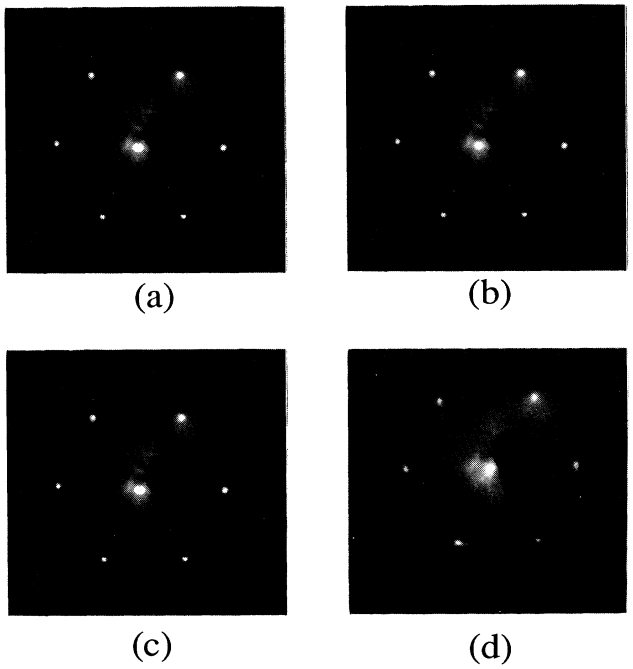

FIG. 1. Diffraction patterns for the substrate and overlayer with RHEED results in the left and LEED in the right panels: (a) and (b) are for the Ag(111) surface, and (c) and (d) are for 2 ML of Fe(110) on Ag(111).

After about 1500 Å of Ag was deposited, the surface was sputtered by 5-keV Ar^+ ions for a few minutes and annealed at 900 K for half an hour; then the film was cooled back down to 450 K and another 100–200 Å of Ag was epitaxially grown onto the surface. After this process, a flat Ag(111) surface was achieved as indicated by the high-quality RHEED and LEED patterns shown in Fig. 1. The RHEED spots, which lie in a semicircle, the Kikuchi lines in the RHEED background, and the relatively sharp LEED spots are characteristic of an ideal, flat surface. It should be emphasized that the processes of sputtering, annealing, and homoepitaxy are important to improve the Ag(111) surface quality. The Fe(110) film was deposited onto the Ag(111) surface from an Fe foil in an alumina crucible; the deposition rate was 0.1 Å/min and the substrate temperature was again 450 K. The pressure during the growth process remained below 3×10^{-10} Torr. The growth of Fe(110) on Ag(111) was monitored *in situ* using the 350-eV Ag Auger signal, as shown in Fig. 2. The Fe film thickness was determined independently from a quartz-crystal thickness monitor. The polygonal shape and kinks at the completion of each monolayer in the Auger data in Fig. 2 suggest that the growth mode is layer by layer. The RHEED and LEED patterns for a 2-ML Fe(110) film are shown in Figs. 1(c) and 1(d). Although the diffraction patterns are not as good as for the Ag, the sharp RHEED streaks and LEED spots indicate that a single-crystal Fe(110) film formed

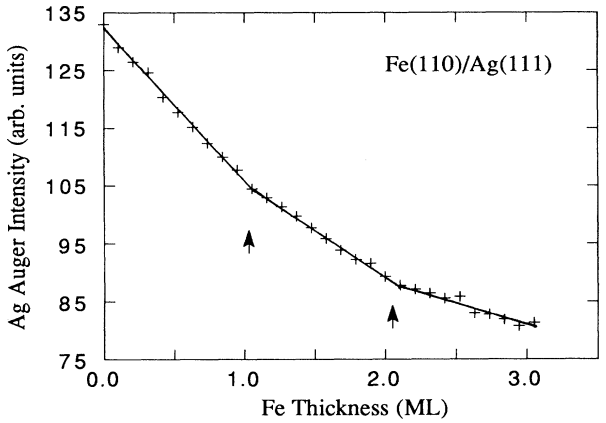

FIG. 2. The 350-eV Ag Auger peak intensity as a function of Fe film thickness. The kinks suggest a layer-by-layer growth mode for Fe(110) on Ag(111).

with only atomic-scale roughness.

The magnetic properties of the films were studied *in situ* by means of the SMOKE technique. Linearly polarized light from a He-Ne laser was used at an angle of incidence of 20°; an analyzing polarizer was set 2° from extinction, and a quarter-wave plate was used to remove the birefringence of the UHV window. The light intensity detected by a photodiode, referred to as the Kerr intensity, was recorded as a function of the applied magnetic field H. H was applied in the film plane and in the plane of incidence of the light (longitudinal Kerr effect) along Ag[11$\bar{2}$] directions. Figure 3 shows a typical set of SMOKE signals from a 2-ML Fe(110) film. The hysteresis loops have remanence and a low coercivity at low

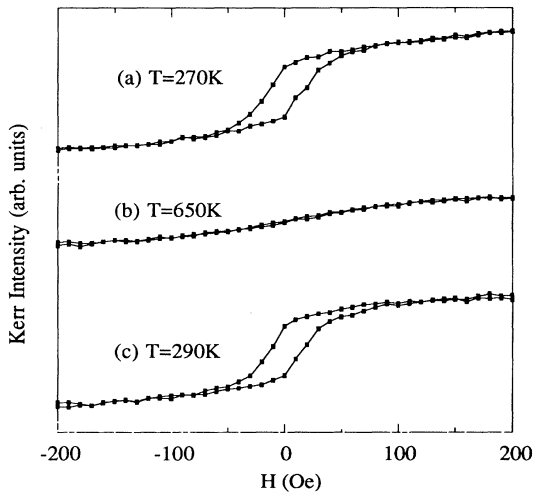

FIG. 3. A sequence of longitudinal-Kerr hysteresis loops for 2 ML of Fe that exhibits the thermal reversibility of the system: (a) 270 K before heating, (b) 650 K, (c) after cooling back to 290 K.

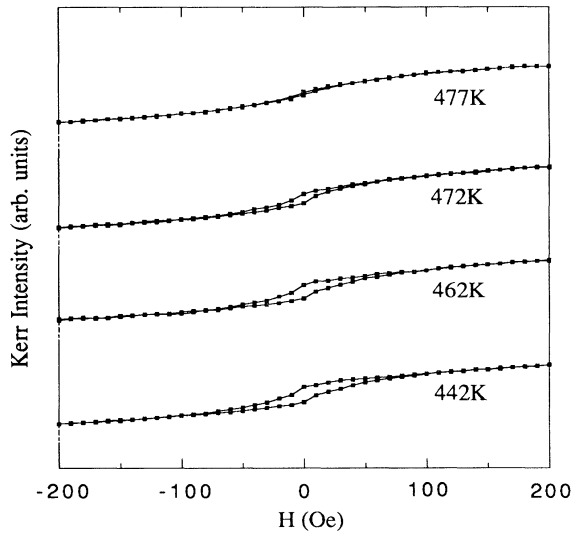

FIG. 4. The longitudinal Kerr signal for 2 ML of Fe in the vicinity of T_C.

temperature, indicative of easy axes of magnetization in the film plane, consistent with previous Mössbauer observations for the Fe/Ag(111) system [19]. It is important to note that the hysteresis loops in Fig. 3 are reversible upon thermal cycling, in sharp contrast to the systems Fe/Cu [21] and Fe/Au [16] in which diffusion can take place at elevated temperature.

Typical hysteresis loops in the vicinity of T_C are shown in Fig. 4 for the 2-ML Fe film. T_C is defined here as the temperature at which the remanent Kerr intensity vanishes. The thickness dependence of T_C is depicted in Fig. 5. Note that the T_C values are significantly reduced from the bulk value, in agreement with theoretical expectation and experimental results for other systems [10–12]. The lack of a measurable transition in the 1-ML range is probably associated with the onset of superparamagnetism, as was observed in the Fe/Ag(111) Mössbauer studies below 2 ML [20]. Alternatively, the loss of anisotropy could suppress T_C. A linear extrapolation of the data from above 2 ML thickness that yields a zero intercept is included in Fig. 5.

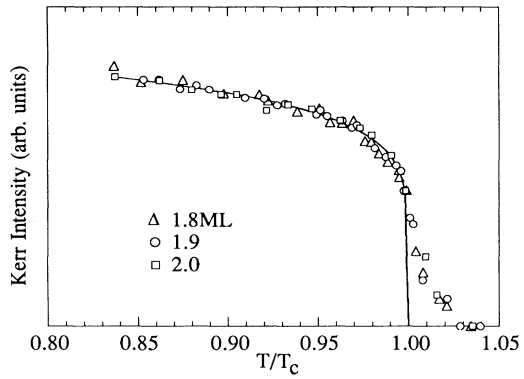

FIG. 6. A magnetization plot of the phase transition constructed from the remanent Kerr intensities vs T/T_C for the indicated Fe film thicknesses.

In order to study the magnetic phase transition, we examined the remanent Kerr intensity near T_C for films with Fe thicknesses of 1.8, 1.9, and 2.0 ML. Since the Kerr intensity is proportional to the magnetization, we can fit our data with the power-law expression for M with T_C and β as parameters. Figure 6 shows the raw data and fitted curve for the three films. Note the films each show a second-order phase transition with universal behavior. There is also an $\sim$3% tail above the fitted T_C value, due to the finite-size effect [22,23] from surface defects and steps that physically limit the correlation length ξ from diverging. If the critical correlation length is given [23] by $\xi_c = \xi_0(1 - T/T_C)^{\nu}$, where ξ_0 is approximated by the lattice constant, and ν is assumed to have the 2D Ising value of 1, we estimate $\xi_c \sim 100$ Å from the

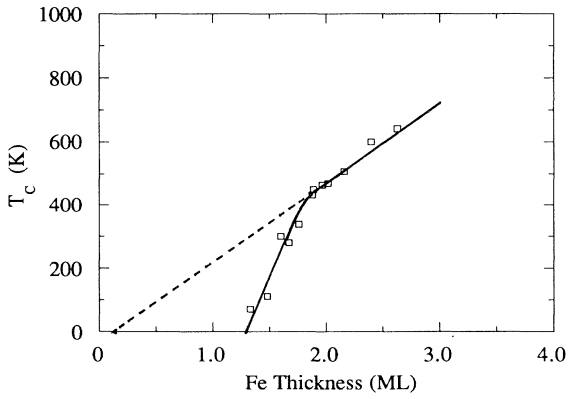

FIG. 5. The thickness dependence of T_C for Fe(110) films on Ag(111), including an interpolation curve (solid) and a linear extrapolation of the $\geq$ 2-ML data (dashed).

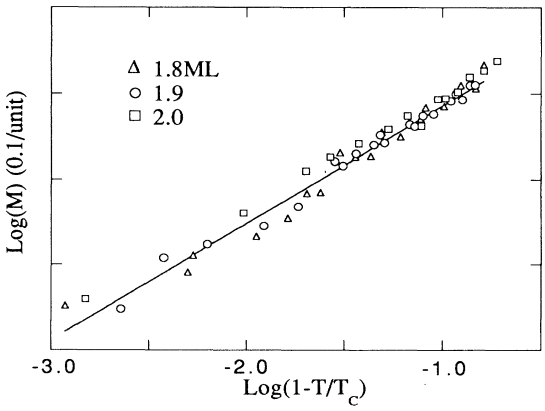

FIG. 7. The log-log plot of the data from Fig. 6, where the slope of the straight line gives the effective β value of 0.137 ± 0.008.

3% tail of our data. This value lies in the same range estimated for Fe/Au(100) [11]. Furthermore, the fact that the film thickness is much smaller than ξ_C implies that the phase transition is two dimensional. Figure 7 shows a log-log plot of the remanent Kerr intensity versus $1-T/T_C$. The slope of the straight line is used to define the effective β value. The average value for the three films is 0.137 ± 0.008, and the individual determinations yield 0.139 ± 0.006, 0.139 ± 0.004, and 0.130 ± 0.003 for the 1.8-, 1.9-, and 2.0-ML films whose fitted T_C values are 338.1, 450.5, and 466.4 K, respectively. The relative thickness independence of β compared to T_C reflects the universality of β which comes from the dimensionality of the system. Our β value is in the range expected theoretically for 2D phase transitions, and is very close to the 2D Ising value of $\frac{1}{8}$. The very slight enhancement of β over $\frac{1}{8}$ may be a consequence of the finite-size effect, since any rounding of M vs T near T_C could increase the value of β [22]. We tested the sensitivity of our β value to the temperature interval used in the fitting procedure. If we limit the range to within only 5% of T_C, only half the points are retained in the fit, but we still obtain $\beta=0.133\pm0.008$. The reason that the transition for Fe(110)/Ag(111) is Ising class is that Fe(110) has only twofold rotational symmetry in the plane of the film, and the in-plane surface magnetic anisotropy, as analyzed by Gradmann, Korecki, and Waller [24], yields two-state switching. The in-plane surface anisotropy, however, is expected to vanish, to second order in M, if the system possesses greater than twofold rotational symmetry [24]. This may help explain why Ising behavior was not observed in Refs. [13] and [14], while it is observed for systems with perpendicular spin orientations, like Fe/Pd(100) [12].

In summary, we have successfully grown Fe(110)/Ag(111) films by MBE. RHEED, LEED, and Auger characterizations reveal that our films are high-quality, single crystals with only atomic-scale roughness. The SMOKE technique was applied *in situ* to study the magnetic phase transition in the Fe thickness range of 1–3 ML. We found that the magnetization of Fe undergoes a 2D second-order phase transition with thickness-dependent T_C values that are significantly reduced from the bulk value. The effective magnetization exponent β is 0.137 ± 0.008, in good agreement with the theoretical value of the critical exponent β_c of $\frac{1}{8}$ predicted by the 2D Ising model.

The work was supported by U.S. Department of Energy, Basic Energy Sciences–Materials Sciences, under Contract No. W-31-109-ENG-38.

[1] See, for example, L. M. Falicov *et al.*, J. Mater. Res. **5**, 1299 (1990); F. Gautier, Mater. Sci. Forum. **59&60**, 361 (1990).
[2] M. D. Mermin and H. Wagner, Phys. Rev. Lett. **17**, 1133 (1966).
[3] M. Bander and D. L. Mills, Phys. Rev. B **38**, 12015 (1988).
[4] F. Y. Wu, Rev. Mod. Phys. **54**, 235 (1982).
[5] C. N. Yang, Phys. Rev. **85**, 808 (1952).
[6] M. Suzuki, Prog. Theor. Phys. **37**, 770 (1967); J. Tobochnik, Phys. Rev. B **26**, 6201 (1982).
[7] J. M. Kosterlitz and D. J. Thouless, J. Phys. C **6**, 1181 (1973); J. M. Kosterlitz, J. Phys. C **7**, 1046 (1974).
[8] J. V. José *et al.*, Phys. Rev. B **16**, 1217 (1977); for weak random anisotropy see B. Dieny and B. Barbara, Phys. Rev. B **41**, 11549 (1990).
[9] S. D. Bader, Proc. IEEE **78**, 909 (1990).
[10] M. Stampanoni *et al.*, Phys. Rev. Lett. **59**, 2483 (1987).
[11] W. Dürr *et al.*, Phys. Rev. Lett. **62**, 206 (1989).
[12] C. Liu and S. D. Bader, J. Appl. Phys. **67**, 5758 (1990).
[13] C. Rau, Appl. Phys. A **49**, 579 (1989).
[14] C. A. Ballentine *et al.*, Phys. Rev. B **41**, 2631 (1990).
[15] R. L. Fink *et al.*, Phys. Rev. B **41**, 10175 (1990); M. Stampanoni *et al.*, Phys. Rev. B **37**, 10380 (1988).
[16] C. Liu and S. D. Bader, J. Vac. Sci. Technol. **8**, 2727 (1990).
[17] S. Blügel, M. Weinert, and P. H. Dederichs, Phys. Rev. Lett. **60**, 1077 (1988).
[18] C. L. Fu, A. J. Freeman, and T. Oguchi, Phys. Rev. Lett. **54**, 2700 (1985).
[19] C. J. Gutierrez, S. H. Mayer, and J. C. Walker, J. Magn. Magn. Mater. **80**, 299 (1989).
[20] Z. Q. Qiu *et al.*, Phys. Rev. Lett. **63**, 1649 (1989).
[21] C. Liu, E. R. Moog, and S. D. Bader, Phys. Rev. Lett. **60**, 2422 (1988).
[22] D. P. Landau, Phys. Rev. B **13**, 2997 (1976).
[23] M. N. Barber, in *Phase Transitions and Critical Phenomena,* edited by C. Domb and J. L. Lebowitz (Academic, New York, 1983), Vol. 8.
[24] U. Gradmann, J. Korecki, and G. Waller, Appl. Phys. A **39**, 101 (1986).

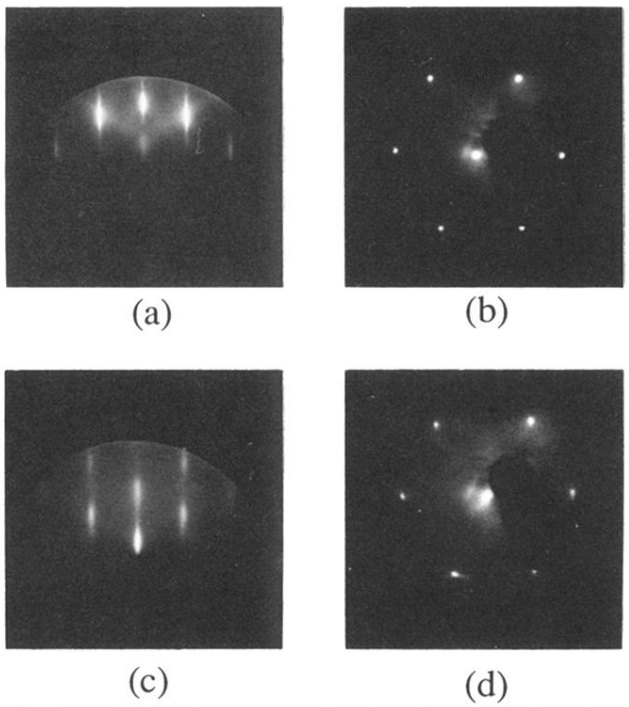

FIG. 1. Diffraction patterns for the substrate and overlayer with RHEED results in the left and LEED in the right panels: (a) and (b) are for the Ag(111) surface, and (c) and (d) are for 2 ML of Fe(110) on Ag(111).